# J12.2 IMPACT OF LAND USE CHANGE ON THE REGIONAL CLIMATE OF MOUNT KILIMANJARO

Jonathan G. Fairman Jr. *
The University of Alabama in Huntsville, Huntsville, Alabama

Udaysankar S. Nair
Earth System Science Center, Huntsville, Alabama

Sundar A. Christopher
The University of Alabama in Huntsville, Huntsville, Alabama

## 1. INTRODUCTION

Impact of land use may be important for the regional climate of Mt. Kilimanjaro in East Africa, where retreat of glaciers on the Kibo Peak has been linked to global climate change (Thompson et al., 2002). Studies by Lawton et al., (2002); Nair et al., (2003) and Ray et al., (2006) show changes in orographic cloudiness at other locations such as Monteverde, Costa Rica in response to deforestation at lower elevations. Similarly, deforestation at lower elevations of Mt. Kilimanjaro could impact orographic cloudiness at higher elevations, thereby altering insolation, precipitation at its peaks and thus the glacier mass balance.

However, the response to deforestation at Mt. Kilimanjaro could be substantially different to that found in prior studies over Costa Rica due to the different geographical settings. Monteverde, Costa Rica is part of a long chain of mountains along the continental divide where the orographic cloudiness is caused by the interaction of trade winds with the terrain. Mt. Kilimanjaro, on the other hand, is an isolated terrain feature in a continental setting where mesoscale numerical modeling experiments by Mölg et al. (2006) suggest that terrain-generated convection may be as or more relevant than cloud formation due to the direct topographical lifting of air. The primary goal of this study is to examine the sensitivity of terrain-generated convection to deforestation along the slopes of Mt. Kilimanjaro.

The Regional Atmospheric Modeling System (RAMS; Cotton et al. 2003) was used to conduct numerical simulations examining the sensitivity of terrain-generated convection to deforestation in the vicinity of Mt. Kilimanjaro. A brief description of the methodology used in this experiment is given in section 2, while evaluation of the model performance and results from the sensitivity analysis are given in sections 3 and 4, with conclusions presented in section 5.

* *Corresponding author address:* J.G. Fairman Jr., The University of Alabama in Huntsville, 320 Sparkman Drive, Huntsville, AL 35801
e-mail: fairman@nsstc.uah.edu

## 2. METHODOLOGY

This study utilizes RAMS simulations for the period 1-31 July 2007, to conduct sensitivity analyses for three differing land use scenarios: current land use scenario (CTL), a pristine reforested case (REF), and a deforested case (DEF). The dry season month of July is used in the experiment since the local orographic convection is expected to dominate over large-scale forcing.

### 2.1 MODEL CONFIGURATION

All three experiments use a hierarchy of four nested grids. The outermost grid has a 64 km grid spacing and a domain that includes a substantial portion of east Africa and the Indian Ocean (Figure 1). Three interior nested grids of progressively decreasing grid spacing are used to establish a domain with grid spacing of 1 km covering Mt. Kilimanjaro.

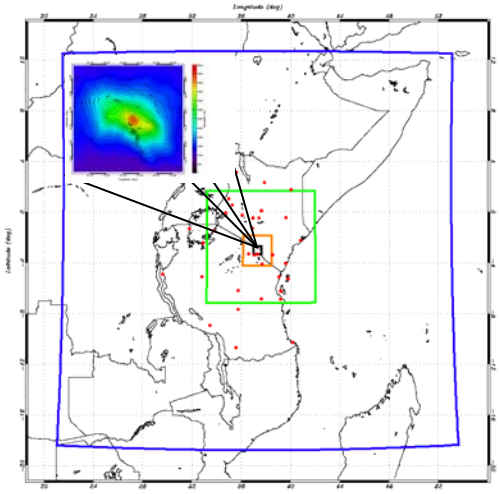

Figure 1: Diagram of nested grids for this experiment: blue for Grid 1 (64 km), green for Grid 2 (16 km), orange for Grid 3 (4 km) and black for Grid 4 (1 km). Red dots indicate surface weather stations used for model verification, and inset shows Grid 4 topography.

In the vertical, 45 levels are used, with the grid spacing increasing by a factor of 1.08 from 60 m at the lowest level to 1 km higher up in the atmosphere. The study analysis will focus on the innermost grid with one kilometer grid spacing where explicit microphysical parameterization is used to represent cloud and precipitation processes.

RAMS is integrated for 24 hours each day of July starting with initial atmospheric conditions specified using three-dimensional Global Forecast System (GFS-ANL) 1° x 1° analysis of wind, temperature, and moisture fields at 0 UTC. The lateral boundaries and the model top are constrained by nudging it towards conditions consistent with the temporally-varying GFS analysis fields available every 6 hours. This experimental design, consistent with the Type I dynamic downscaling classification of Castro et al. (2005), is chosen to retain realism of the large-scale atmospheric conditions around the study area at this time.

However, the soil moisture and temperature conditions in the RAMS experiments are initialized from GFS analysis only once, at 0 UTC of 1 July 2007. Thus, unlike the atmospheric conditions which are reinitialized every 24 hours, soil moisture and temperature is allowed to continuously evolve in all the experiments during the entirety of the study period. This approach retains the evolution of the finer-scale features of the land boundary conditions that have a longer memory compared to atmospheric conditions.

### 2.2 LAND USE SCENARIOS

Land cover in the CTL experiment (Figure 2a) is specified using the Olson Global Ecosystem (OGE) dataset, the default land cover characterization dataset used by RAMS (Loveland et al. 2000). In the DEF experiment, all evergreen and deciduous forest areas (which constitute 13.3% of the total area of the grid) as well as wooded grassland areas (which constitute 53.5% of the area of the grid) are converted to short grass, extending the extremes of deforestation found along the western and northern slopes found in the CTL experiment (Figure 2b). While the arbitrary conversion of 53.5% of the total land cover from wooded grassland may not be realistic, it provides an upper bound for the effects of land use change. In the REF experiment (Figure 2c), all the current areas that are farmland or urbanized, which constitute 14.4% of the grid are replaced by evergreen forests to match the land cover found at the middle elevations in CTL experiment.

In the CTL scenario, the spatial distribution of NDVI is specified using a more representative MODIS-Terra-derived NDVI data set from July of 2007 rather than the default AVHRR-derived NDVI dataset used by RAMS. In the DEF and REF scenarios, average values of NDVI of the altered land use classifications were used. For example, an average NDVI for the evergreen forested class, determined from the MODIS NDVI data used in the CTL experiment, is used to specify the NDVI for evergreen forest that replaces urban or farmland regions in the REF case.

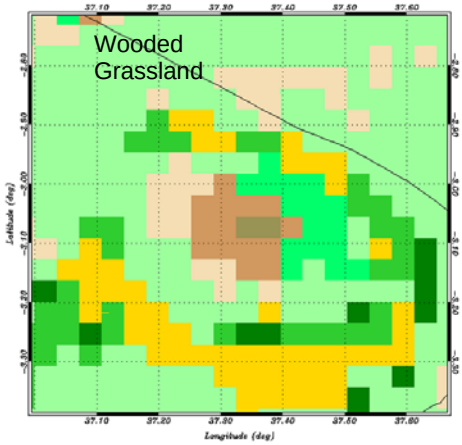


Figure 2a: Control land use scenario.

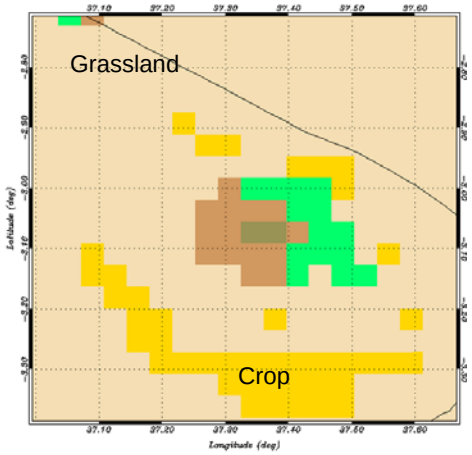


Figure 2b: Deforested land use scenario.

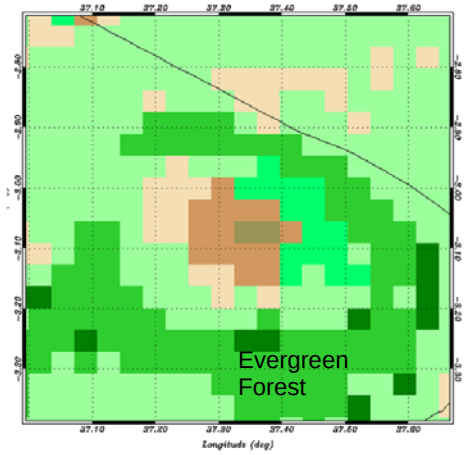


Figure 2c: Reforested land use scenario.

## 3. EVALUATION OF NUMERICAL MODEL PERFORMANCE

To evaluate the numerical model performance, Root Mean Square Error (RMSE), Bias, and (BIAS) Error Standard Deviation (ESD) were computed utilizing hourly surface meteorological observations and simulated values at the grid point closest to the location of the observation in the second grid (G2) of CTL simulation. RMSE, BIAS, and ESD provides overall quantification of error, information regarding systematic errors (such as model parameterizations) and information about non-systematic errors (boundary conditions errors), respectively. Since East Africa is a relatively observation-poor area, only a few stations with observational fidelity sufficient for statistical analysis exist within the domain covered by the model grids. The second grid that covers approximately half of both Tanzania and Kenya provides the maximum number of comparisons between observations and simulation.

The comparisons indicate that the computed values of RMSE, BIAS, and ESD (Table 1) all fall within ranges reported by modeling studies over other regions (Zhong and Fast 2003, Miao et al. 2007, Mölders 2008), demonstrating adequate performance of RAMS over the study area.

| | |
|---|---|
| 2 m Temperature RMSE | 2.02 K |
| 2 m Temperature Bias | –1.38 K |
| 2 m Temperature ESD | 2.56K |
| Dewpoint RMSE | 0.94 K |
| Dewpoint Bias | –0.24 K |
| Dewpoint ESD | 1.34 K |

Table 1: Two meter temperature and dewpoint model statistics from comparisons to observations.

## 4. RESULTS

The RAMS simulations, assuming the three different land use scenarios, were compared to examine the differences in downwelling shortwave radiation, orographic cloudiness, terrain-induced flow patterns, precipitation and also surface temperature and moisture patterns. Substantial differences were found between the three scenarios, with implications for observed changes occurring at Mt. Kilimanjaro.

### 4.1 DOWNWELLING SHORTWAVE RADIATION

Downwelling shortwave radiation at the surface is one of the primary factors that impact glacier mass balance. In this context, the overall impact of land use change on downwelling shortwave radiation at the top of Mt. Kilimanjaro is important, where glaciers exist at altitudes exceeding 5000 m. Downwelling shortwave radiation, averaged at grid points in the model domain over 5000 m, show significant differences between the CTL, DEF, and REF experiments during a good portion of the day (Figure 3). Differences in excess of –50 W $m^{-2}$ are found to occur between the DEF and CTL simulations at local noon, with the diurnally-averaged shortwave radiative forcing exceeding –6 W $m^{-2}$. This means that there is less downwelling shortwave radiation at the peak of Mt. Kilimanjaro throughout the day in the deforested scenario. The peak average differences of 15 W $m^{-2}$ exist between the REF and the CTL experiments, with the diurnally-averaged difference being +3.4 W $m^{-2}$. The experiments demonstrate a consistent pattern where the downwelling shortwave radiation at the peak of Mt. Kilimanjaro reduces with an increase in the level of deforestation at the lower elevations, suggesting that deforestation alters the frequency and composition of clouds over upslope areas.

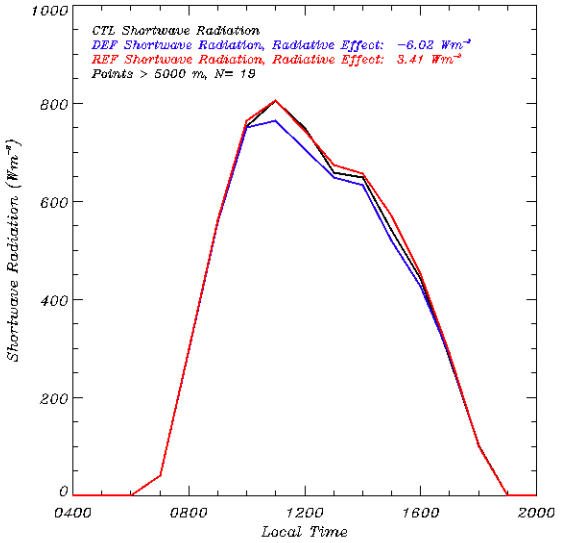


Figure 3: Diurnally-averaged downwelling shortwave radiation at points above 5000 m in elevation for the three differing runs.

### 4.2 OROGRAPHIC CLOUD FORMATION

Comparison of cloudiness from the Moderate Resolution Imaging Spectroradiometer (MODIS) morning and afternoon overpasses to cloudiness from the CTL simulations at the hour closest to the overpass time, show relatively good qualitative agreement (Figure 4). Similar to MODIS observations (Figure 4a, 4c), the CTL simulation shows two arcs of high cloudiness on the windward and lee slopes of Kilimanjaro (Figure 4b, 4d). The CTL simulation exhibits a tendency to over predict the frequency of occurrence of cloudiness (FOC) over the peaks of Kilimanjaro compared to MODIS observations. However, note the comparison is not exact since the model-computed FOC also includes optically thin clouds which will not be detected by the satellite and

the time of comparison is not exact. Table 2 shows the quantitative cloud accuracy for the fine model grid, for both the MODIS-Aqua and MODIS-Terra overpass times. The accuracy listed is for correctly predicting either a cloudy or clear situation. Overprediction is where the model is cloudy and observation is clear; underprediction is the opposite. These numbers are comparable to Ray et al. (2006) for orographic formation within RAMS.

| | Accuracy | Overprediction | Underprediction |
|---|---|---|---|
| Terra | 55.2% | 19.2% | 25.6% |
| Aqua | 57.4% | 18.2% | 24.4% |

Table 2: Model accuracy, overprediction, and underprediction of cloud occurrence at MODIS-Terra and MODIS-Aqua overpasses.

Comparison of spatial distribution of FOC between the three land cover scenarios are consistent with the pattern of differences in downwelling shortwave radiation at the surface. Spatially averaged FOC as a function of altitude shows that FOC initially increases with elevation reaching a maximum at altitudes of ~2500 m (Figure 5a) and then steadily decreases above this altitude. Comparison between the CTL and DEF simulations (Figure 5b) show that impact of deforestation on FOC is to decrease the cloudiness at lower elevations while increasing it at higher altitudes (Figure 5b). Reforestation results in an opposite pattern where it leads to an increase in FOC at lower elevations and a decrease at higher elevations (Figure 5c). Maximum decrease and increase in FOC at lower and higher elevations respectively is found between the DEF and REF simulations (Figure 5d).

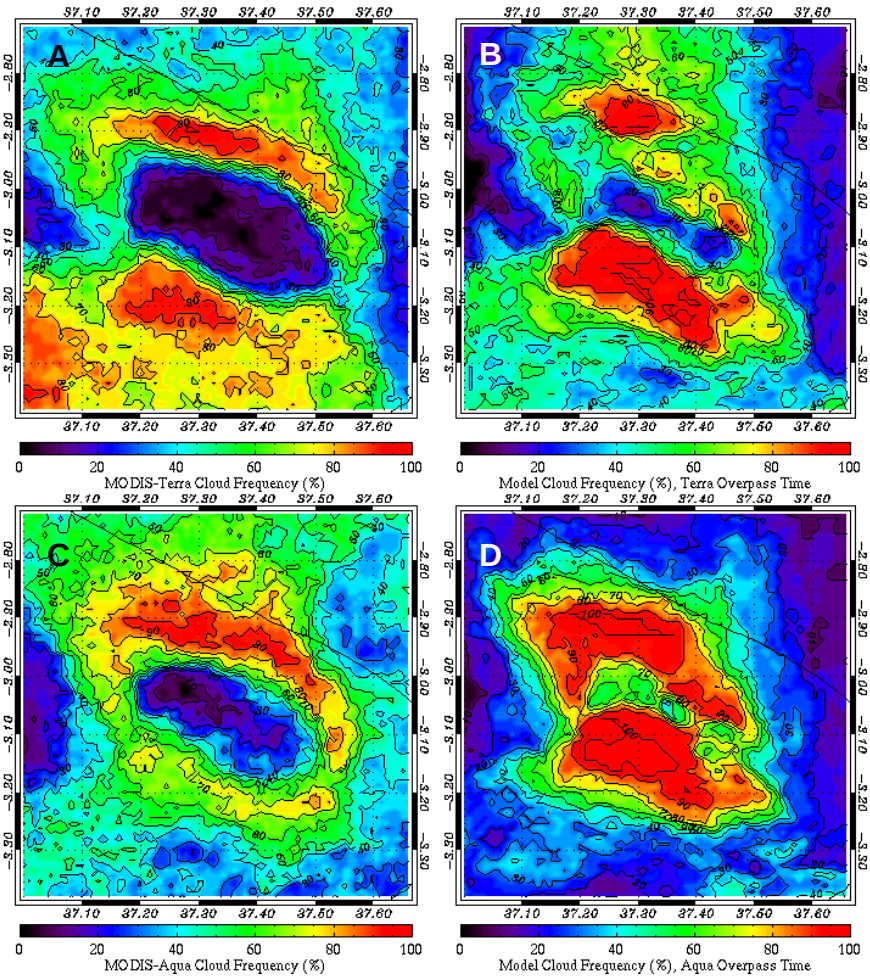


Figure 4: Comparison of MODIS Terra (top left) and Aqua (bottom left) cloud frequency to model cloud frequency (top and bottom right).

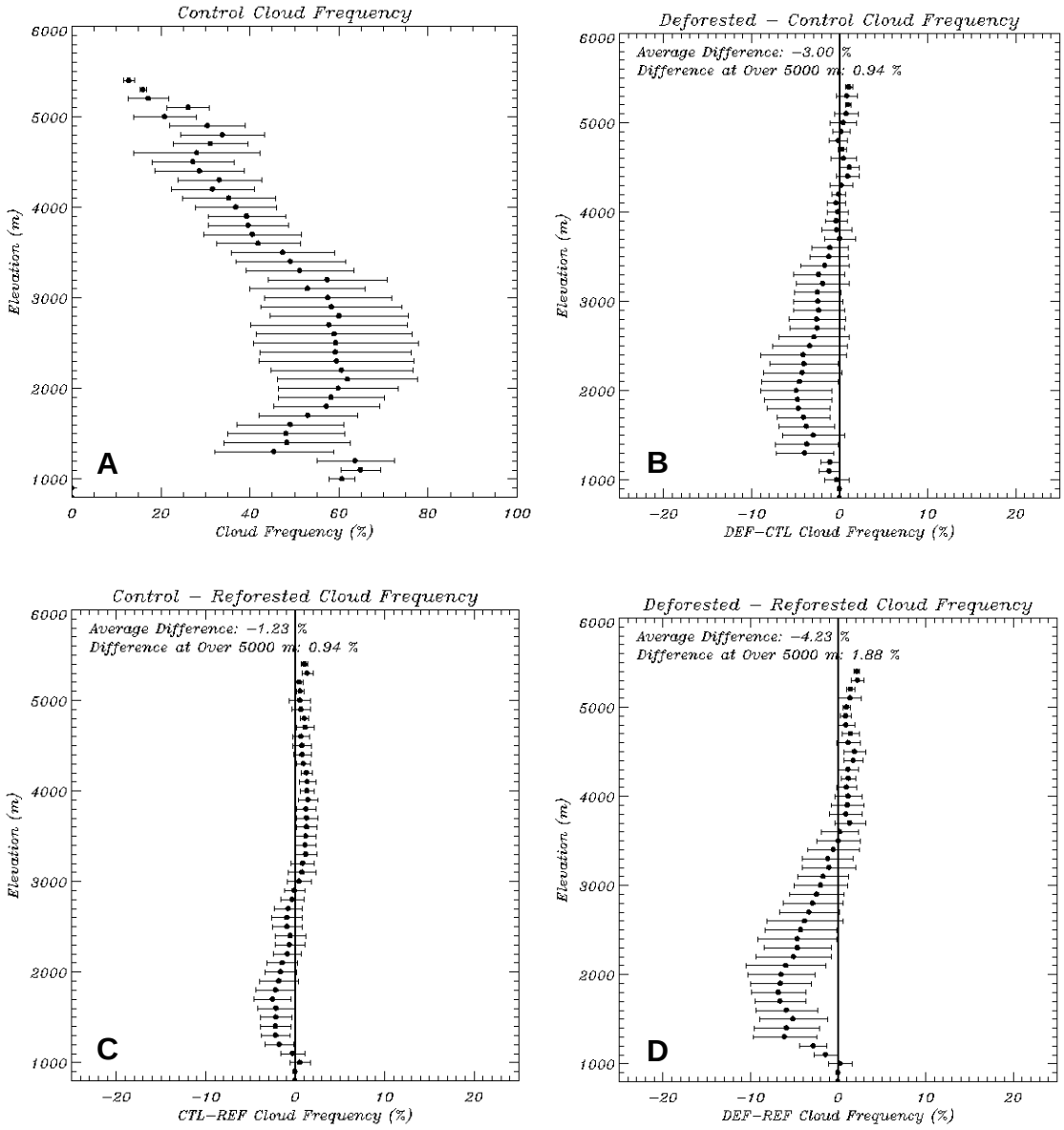


Figure 5: Cloud frequency differences binned to 100 m elevation increments for the one kilometer spacing model grid. Dots indicate mean values and bars indicate plus or minus one standard deviation.

Comparing the different scenarios shows that the variations in the integrated liquid water path (LWP) may play a more significant role than FOC in altering downwelling shortwave radiation at the mountain peak. Whereas there is only a 0.94% difference in cloud frequency over the peak between the DEF and CTL cases, there is an 11% difference in cloud liquid water path over the peak. There is also a 10% deficit in cloud liquid water path between the CTL and REF cases. Therefore, not only are clouds more frequent in the DEF case versus the CTL and REF cases, clouds are also generally thicker at higher elevations. For the entire grid, however, the clouds are thinner for the DEF case, with an average deficit of 4.87 $gm^{-2}$ in cloud liquid water path from the CTL case. On average, the REF case has a 1.92 $gm^{-2}$ increase in cloud liquid water path compared to the CTL case. Therefore, while the clouds over the entire grid are thicker and more frequent as the forested area increases,,the clouds over higher elevation areas are thinner and less frequent. This is most likely due to elevation of the cloud base height over Costa Rica as demonstrated in Nair (2003) and Ray (2006). The area of maximum convection occurs at a higher elevation because of raised lifting condensation levels since there is less moisture available at the surface. Since there is still significant forcing available for convection (as shown in the next section), the total cloud height stays similar and therefore FOC and LWP at higher elevations increase.

### 4.3 WIND PATTERNS

The CTL, DEF and REF simulations also show differences in wind patterns, with increased surface wind speeds along the eastern and westerns slopes of Kilimanjaro (Figure 6). The wind speeds along these slopes are highest in the DEF simulation followed by the CTL and REF simulations. Increase in surface wind speeds are primarily due to smaller roughness length along the eastern and western slopes in CTL and DEF simulations compared to the CTL simulation. The behavior of increasing leeward orographic cloudiness in response to increased deforestation is caused by enhanced leeward convergence resulting from higher surface wind speeds. There is also more upslope flow in the deforested case in comparison to the other two cases, which helps to explain the increases in upslope cloud cover demonstrated in the previous sections.

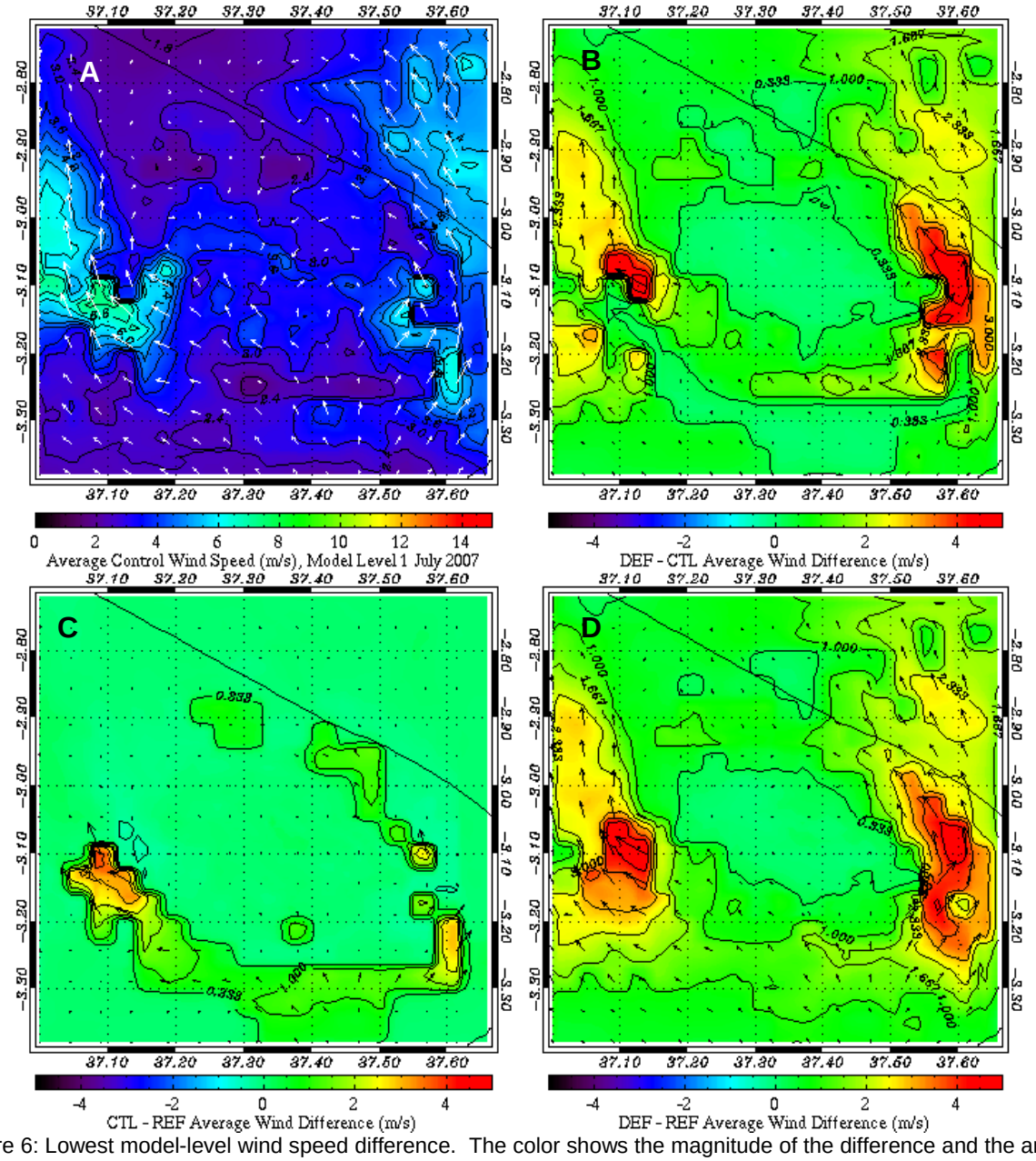


Figure 6: Lowest model-level wind speed difference. The color shows the magnitude of the difference and the arrows show the vector difference.

### 4.4 OROGRAPHIC PRECIPITATION

A spatial average of accumulated precipitation shows an increase with elevation up to an altitude of ~2400 m and then decreases with altitudes up to ~4000 m (Figure 7a). This pattern is consistent with elevational profiles of precipitation reported for Mt. Kilimanjaro (Barry 2008). Above 4000 m, the CTL simulation shows a steady increase in precipitation with height reaching maximum values at the highest elevations. Compared to the CTL simulation, the DEF simulation shows a slight decrease in average precipitation at elevations less than 2200 m and a general increase at higher altitudes with the maximum increases being found at elevations above 5000 m (Figure 7b). Reforestation results in the opposite pattern where there is an increase in precipitation at lower elevations and a decrease in precipitation at elevations in excess of 5000 m (Figure 7c). The tendency for deforestation to decrease precipitation at lower altitudes and increase it at higher altitudes is most amplified when comparing the DEF and REF simulations (Figure 7d). In summary, the simulations show that the impact of deforestation is to cause an increase in precipitation at the highest elevations, but at the expense of precipitation at lower elevations.

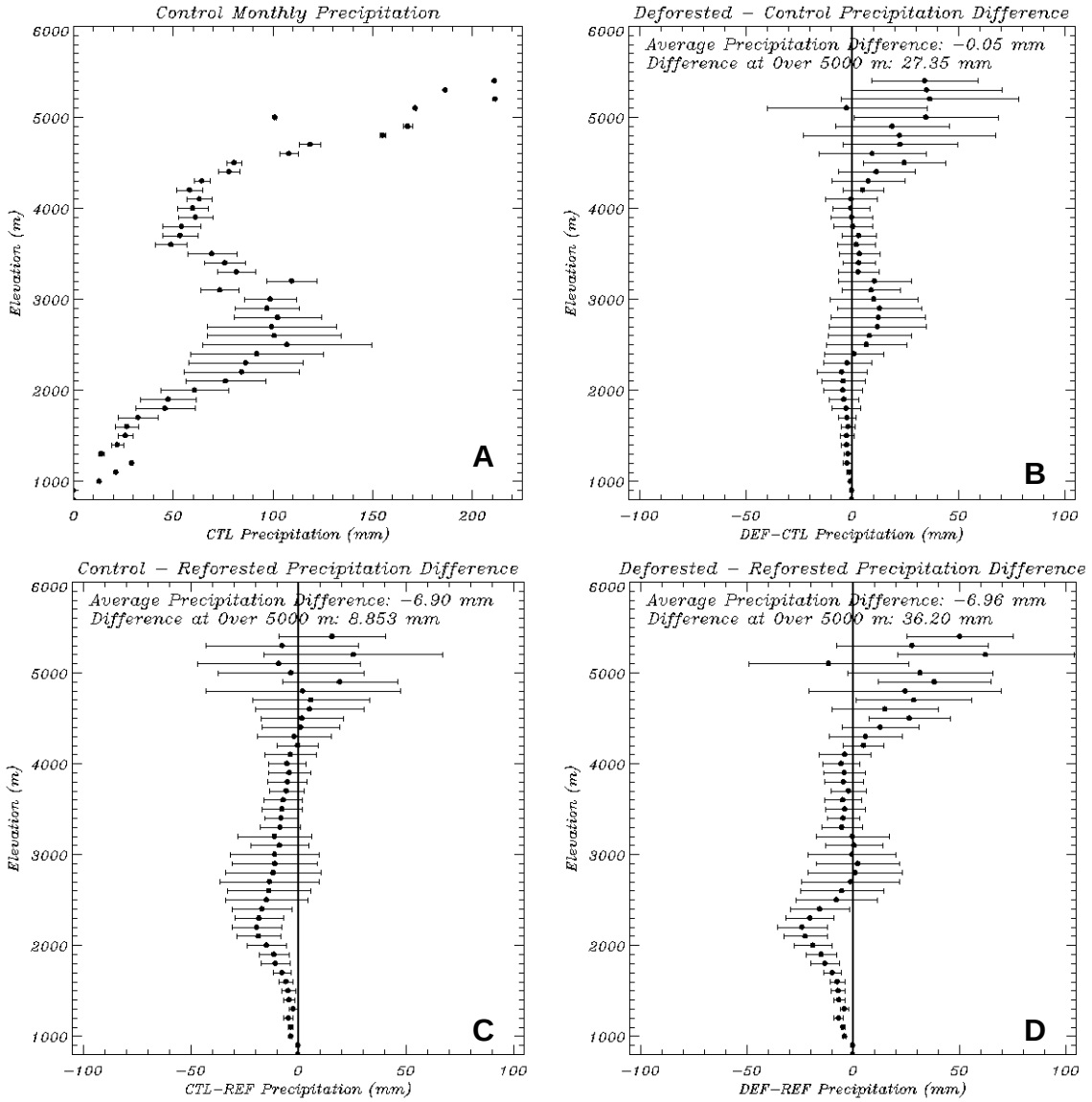


Figure 7: Comparison of surface precipitation with respect to elevation binned at 100 m intervals. The bars indicate a one standard deviation difference from the mean values.

### 4.5 SURFACE TEMPERATURE AND MOISTURE

The DEF simulation shows that the surface air is generally warmer and drier over deforested regions (not shown). The REF simulations show cooler and moister air over forested regions in the windward side. The direct impact of land use change on surface temperature and moisture is difficult to deduce from the simulations since substantial variations in cloud cover are also caused by land cover change.

## 5. CONCLUSIONS

This study investigated the hypothesis that land cover changes at lower elevations of Mt. Kilimanjaro will alter orographic cloudiness, impacting insolation and precipitation at the peak. RAMS simulations of atmospheric conditions for July 2007, assuming current, deforested, and forested land cover scenarios, were used to examine this hypothesis.

The RAMS simulations do indeed show that land cover changes in the vicinity do modulate the nature of orographic cloudiness, with the deforestation increasing cloudiness, liquid water path and precipitation at the peak. The increasing cloudiness in response to deforestation is accompanied by a reduction in downwelling solar radiation at the surface. Total deforestation imposes a diurnally-averaged, shortwave radiative forcing (SWRF) of -6.02 W $m^{-2}$, while reforestation of areas of anthropogenic land cover leads to SWRF of +3.14 W $m^{-2}$ at elevations greater than 5000 m. Simulations assuming deforested and reforested land cover scenarios show that the changes in cloudiness are linked to differences in aerodynamic roughness arising from land cover change. Reforested simulations show a decrease in wind speeds, primarily along regions of reforestation at mid-elevations, enhancing convection in these regions. Deforested simulations exhibit a general strengthening of slope flows, especially along the eastern and western slopes. Since the aerodynamic roughness at lower elevations is reduced, convergence and convection at higher elevations are enhanced. Replacement of areas of anthropogenic land use with forest cover leads to enhanced convergence at mid-elevations. Precipitation at higher elevations is enhanced for the deforested scenario. When averaged over the entire domain, deforestation leads to an overall reduction in precipitation while reforestation causes a small increase.

While land cover change does indeed impact orographic cloudiness at Kilimanjaro, physical mechanisms through which the changes are effected is different than those found in prior studies (Lawton et al., 2002; Nair et al., 2003; Ray et al., 2006; Bruijnzeel, 2004). At Monteverde, Costa Rica, lowland deforestation impacted orographic cloud formation by causing the air mass to be warmer and drier, elevating the lifting condensation level and the height of formation of the orographic cloud bank. In an island setting in Puerto Rico, both changes in air mass and sea-breeze circulation patterns caused by deforestation was found to alter orographic cloudiness (Bruijnzeel, 2004). In the present study the changes appear to be driven mainly by changes in flow patterns caused by alteration of aerodynamic roughness. Also, unlike Monteverde, Costa Rica, where the impact of land use change complements the effects of larger-scale forcing (Pounds et al. 1999), at Kilimanjaro, the present study finds that land use change impacts at the peak mitigate the effects of larger-scale climate variations.


## ACKNOWLEDGEMENTS

Jonathan Fairman was supported by NASA Headquarters under the NASA Earth and Space Science Fellowship Program – Grant NNX08AU74H. Dr. Udaysankar Nair was supported by the NASA NIP Grant NNX06AF09G. Dr. Sundar Christopher was supported by NASA Radiation Sciences Program.


## REFERENCES


Barry, R.G., 2008: *Mountain Weather and Climate*, 3d ed., Cambridge University Press, 512 pp.

Bruijnzeel, L. A., 2004: Hydrological functions of tropical forests: Not seeing the soil for the trees? *Agric. Ecosyst. Environ*., **104,** 185–228.

Bruijnzeel, L. A., and J. Proctor, 1993: Hydrology and biogeochemistry of tropical montane cloud forests: What do we really know? *Tropical Montane Cloud Forests,* L. S. Hamilton, J. O. Juvik, and F. N. Scatena, Eds., East–West Center, 21–46.

Castro, C.L., R.A. Pielke Sr., and G. Leoncini, 2005: Dynamical downscaling: Assessment of value retained and added using the Regional Atmospheric Modeling System (RAMS). *J. Geophys. Res.*, **110**, No. D5, D05108, doi:10.1029/2004JD004721.

Lawton, R. O., U. S. Nair, R. A. Pielke Sr., and R. M. Welch, 2001: Climatic impact of tropical lowland deforestation on nearby montane cloud forests. *Science,* **294,** 584–587.

Mölders, N., 2008: Suitability of the Weather Research and Forecasting (WRF) Model to predict the June 2005 fire weather for interior Alaska. *Weather and Forecasting*, **23**, 953-973.

Miao, J.F., and Coauthors, 2007: Evaluation of MM5 mesoscale model at local scale for air quality applications of the Swedish west coast: Influence of PBL and LSM parameterizations, *Meteor. Atmos. Phys.,* **99**, 77-103.

Mölg, T., N. J. Cullen, D. R. Hardy, and G. Kaser, 2006: Tropical glaciers in the context of climate change and society: Focus on Kilimanjaro (East Africa), *The Darkening Peaks: Glacial Retreat in Scientific and Social Context*, B. Orlove, E. Wiegandt, and B. Luckman, Eds., Univ. of Calif. Press, Berkeley

Nair, U.S., R. O. Lawton, R. M. Welch, and R. A. Pielke Sr., 2003: Impact of land use on Costa Rican tropical montane cloud forests: Sensitivity of cumulus cloud field characteristics to lowland deforestation. *J. Geophys. Res.,* **108,** 4206, doi:10.1029/2001JD001135.

Pounds, J. A., M. P. L. Fogden, and J. H. Campbell, 1999: Biological response to climate change on a tropical mountain. *Nature,* **398,** 611–614.

Pielke, R.A., and Coauthors, 1992: A comprehensive meteorological modeling system—RAMS. *Meteor. Atmos. Phys.,* **49,** 69–91.

Ray, D. K., U. S. Nair, R. O. Lawton, R. M. Welch, and R. A. Pielke Sr., 2006: Impact of land use on Costa Rican tropical montane cloud forests: Sensitivity of orographic cloud formation to deforestation in the plains. *J. Geophys. Res.,* **111,** D02108, doi:10.1029/2005JD006096.

Reinecke, P. A., and D. R. Durran, 2008: Estimating orographic blocking using a Froude number hen the static stability is nonuniform, *J. Atmos. Sci.,* **65***,* 1035–1048.

Thompson, L.G., and Coauthors, 2002: Kilimanjaro ice core records: Evidence of Holocene climate change in tropical Africa, *Science*, **298**, 241-262.

Zhong, S., and J.D. Fast, 2003: An evaluation of the MM5, RAMS, and Meso-Eta models at subkilometer resolution using VTMX field campaign data in the Salt Lake Valley. *Mon. Wea. Rev.*, **131**, 1301- 1322.